MedChemComm

CONCISE ARTICLE

View Article Online
View Journal

Cite this: DOI: 10.1039/c5md00074b

Discovery and optimisation of 1-acyl-2-benzylpyrrolidines as potent dual orexin receptor antagonists†

Jodi T. Williams,* John Gatfield, Catherine Roch, Alexander Treiber, Francois Jenck, Martin H. Bolli, Christine Brotschi, Thierry Sifferlen, Bibia Heidmann and Christoph Boss

Received 20th February 2015,
Accepted 14th April 2015

DOI: 10.1039/c5md00074b

www.rsc.org/medchemcomm

Starting from a thienopiperidine lead compound with high intrinsic clearance in rat and human liver microsomes and low aqueous solubility, a novel series of 1-acyl-2-benzylpyrrolidines were discovered as potent and competitive dual orexin receptor antagonists. Metabolic stability was improved to afford oral exposure, and aqueous solubility was increased by twenty fold, providing compounds suitable for pre clinical evaluation. Compound **27** showed insurmountable antagonism at both orexin 1 and orexin 2 receptor sub types and displayed a comparable sleep-promoting effect in the rat to almorexant and suvorexant.

Introduction

The vertebrate orexin neuropeptide–receptor system plays a pivotal role in the regulation of sleep and wake states as well as emotional states related to stress or reward. The neuropeptides orexin A and orexin B are synthesised by a small number of neurons in the lateral hypothalamus, a brain region involved in arousal, emotional and metabolic regulation and motivated behaviours, *e.g.* feeding.[1–4] Orexin peptides are released at axonal terminals and – pre- or post-synaptically – bind and activate two closely related G protein coupled receptors (GPCR): orexin receptor type 1 (OX_1) and orexin receptor type 2 (OX_2).[5–7] Activated neuronal orexin receptors couple to the Gq/phospholipase C/protein kinase C pathway resulting in cellular depolarisation and increased cytosolic Ca^{2+} concentrations.[8] Thus, orexin receptor signaling is excitatory by enhancing synaptic transmission.

The distribution of OX_1 and OX_2 in mammalian brains is indicative of their important role in the regulation of vigilance states and circadian activity. Orexin-secreting neurons of the lateral hypothalamus project to the basal forebrain, corticolimbic structures, and brainstem, especially to those regions related to sleep/wake regulation (locus coeruleus, raphe nucleus, tuberomammillary nucleus), regions activated in anxiety/stress-related conditions (paraventricular nucleus) as well as regions involved in reward processing and drug abuse (nucleus accumbens, ventrotegmental area).[1,2,9–18] Intracerebellar orexin A and orexin B infusion in rats results in enhanced arousal, delayed onset of REM sleep, and maintenance of cortical activation. Pharmacological inhibition of the orexin system in animal models of insomnia, stress/anxiety and drug abuse has demonstrated a central role of an overactive orexin system in these pathologies and suggests orexin receptors as therapeutic targets in insomnia, stress/anxiety-related disorders and addiction.[19–30] Extensive clinical trials with two dual orexin receptor antagonists (DORAs) have demonstrated that targeting the orexin system is an effective strategy in treating sleep disorders. In insomnia patients, both almorexant and suvorexant dose-dependently increased sleep efficiency by decreasing latency to persistent sleep and wake after sleep onset.[31–33] Suvorexant received FDA marketing authorization in 2014 and represents the first-in-class dual orexin receptor antagonist for the treatment of insomnia characterised by difficulties with sleep onset and/or sleep maintenance.[34,35] Studies into the respective contributions of pharmacologically blocking OX_1 and OX_2 on sleep–wake states have revealed a more important role for OX_2.[36] Recent reports describing OX_2 subtype-selective antagonists suggest that blockade of OX_2 alone may be suitable for the treatment of sleep disorders, and future clinical studies should shed light on whether there is an advantage of selectively blocking OX_2 over dual OX_1 and OX_2 blockade.[37,38]

The ideal profile of a sleep drug from a pharmacokinetic perspective is difficult to achieve. Metabolic stability in particular needs to be carefully assessed; too stable runs the risk of overshooting with the pharmacodynamic effect and could lead to "hangover" phenomena. Too unstable, on the other hand, will lead to lower bioavailability and higher doses may be required to achieve the required duration of action. The

Drug Discovery Chemistry, Actelion Pharmaceuticals Ltd., Gewerbestrasse 16, CH-4123, Switzerland. E-mail: jodi.williams@actelion.com

† Electronic supplementary information (ESI) available. See DOI: 10.1039/c5md00074b

latter is then associated with a greater risk for safety findings. It is increasingly recognised that the rate at which a drug associates with and dissociates from its target receptor – its binding kinetics – directly affects the drug's efficacy and safety. In the context of orexin receptor antagonism and sleep, a desired compound profile may be characterised by relatively slow receptor dissociation kinetics eliciting insurmountable antagonism to allow it to also be effective with increasing orexin peptide concentrations. These two independent features of a potential novel sleep drug, namely pharmacokinetic profile and binding kinetics, need to be carefully evaluated to identify the appropriate balance.

In this manuscript, we describe the structural optimisation of our initial lead compound **1** into the *in vivo* active compound 27. During the optimisation process, we focus on OX_2 potency and monitor the lipophilic ligand efficiency (LLE) metric to assess design progress.[39] DORA 27 shows single digit nM potency at both OX receptors and exhibits insurmountable antagonism in calcium release assays at OX_1 and OX_2. An investigation into the binding kinetics of 27 reveals an estimated receptor occupancy half-life of 1–5 min at both orexin receptor subtypes. DORA 27 decreases wakefulness and increases sleep efficiency in male Wistar rats after oral administration of 100 mg kg^{-1}.

Results and discussion

The efforts described herein began with racemic *N*-acylthienopiperidine **1** (Scheme 1), a dual orexin receptor antagonist that we disclosed earlier.[40] DORA **1** showed single digit nM potency at both OX receptors but suffered from poor *in vitro* ADME and physicochemical properties (Table 1). Our initial investigation centred on reducing the lipophilicity of DORA **1** as a means of modulating the high *in vitro* metabolic clearance as determined experimentally in the presence of rat and human liver microsomes (RLM, HLM).

As we considered the thiophene moiety present in **1** a metabolic liability,[41] we eliminated this ring leading to compound **2** (Scheme 1). The removal of the thiophene ring resulted in only a modest 5-fold loss in potency at OX_1; however, a more pronounced 70-fold loss in potency at OX_2 was observed. In the thienopiperidine series, the indole moiety was required to obtain low nM potency at both OX receptors. Attempts to replace it with an *ortho*-biaryl motif, a common feature of many orexin receptor antagonists,[42–45] to give compound **3**, led to a 24-fold and a 300-fold loss in potency at OX_1 and OX_2, respectively. Having removed the thiophene from **1**, we explored the possibility that we would have greater flexibility in terms of acylating the piperidine

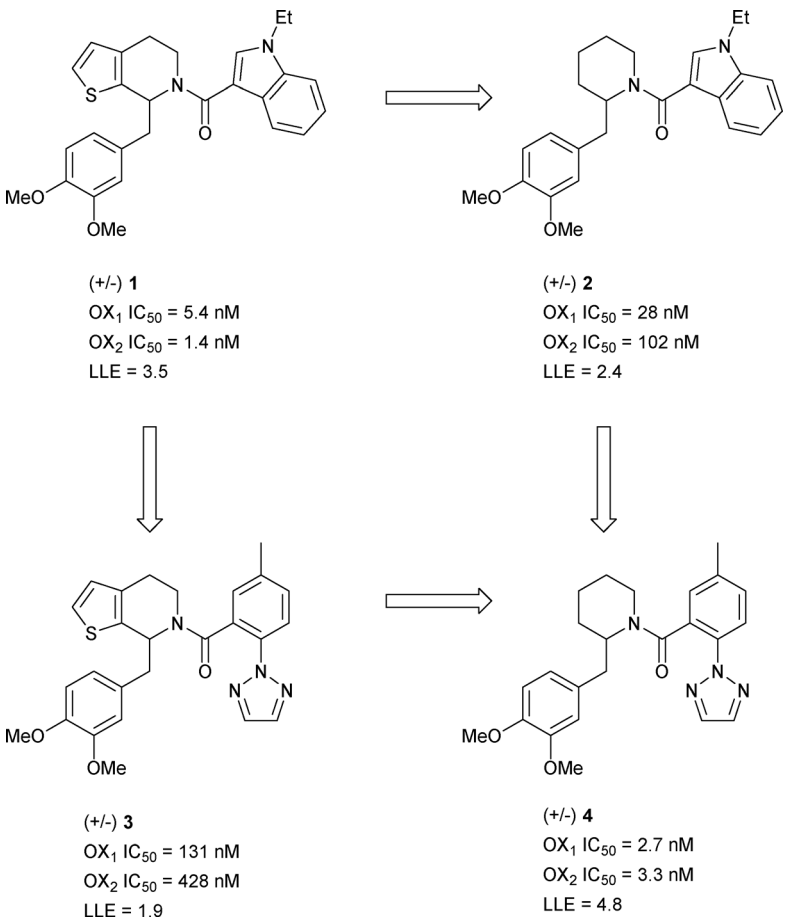

Scheme 1 Initial strategy for reducing lipophilicity of lead compound **1**.

Table 1 Properties of racemic thienopiperidine lead compound **1**

hOX_1 IC_{50}[a]	5.4 nM	MW	460
hOX_2 IC_{50}[a]	1.4 nM	*c* log *P*	5.5
HLM CL_{int}[b]	>1250 μL min^{-1} mg^{-1}	LLE[d]	3.5
RLM CL_{int}[b]	>1250 μL min^{-1} mg^{-1}	Solubility[e]	7 μg mL^{-1} (pH 4.1)
CYP3A4[c] IC_{50}	3 μM		

[a] Geomean of at least 3 experiments, standard deviation is <50% in all cases. [b] Intrinsic metabolic clearance with liver microsomes, at 1 μM. [c] Testosterone 6β-hydroxylation used as a P450 isoform-specific marker. [d] Calculated from hOX_2 IC_{50}. [e] Water, unbuffered.

nitrogen and we prepared the piperidine analog of compound **3**. To our delight, this modification resulted in DORA **4** showing single digit nM potency at both OX receptors.

The LLE metric is used to capture the efficiency of improved *in vitro* potency in relation to change in lipophilicity: LLE = pIC_{50} − *c* log *P*. It has been proposed that an acceptable target LLE for a drug candidate lies in the region >5.[46] The modifications leading to **4** clearly were steps in the right direction in terms of addressing the poor physicochemical properties highlighted for DORA **1**. LLE was improved (4.8 *vs.* 3.5), molecular weight was lower (420 *vs.* 460) and there was a measurable improvement in intrinsic clearance in HLM (CL_{int} 616 *vs.* >1250).

We next explored modifications of the benzyl group at the 2-position of the piperidine ring (Table 2). Extending to the phenethyl analog **5** led to a 10-fold and a 5-fold loss in potency at OX_1 and OX_2, respectively. Subsequent removal of the 4-methoxy substituent led to a further loss in potency as illustrated by compound **6**. Intrinsic clearance in HLM was measured for compounds **5** and **6** and offered no advantage over **4**. Given the apparent preference for benzyl over phenethyl in terms of potency, we chose to keep the benzyl group in further optimisation efforts.

All compounds that have been described so far were prepared as racemates. The next modification that was investigated was ring contraction of the piperidine to the corresponding pyrrolidine. This modification gave us the opportunity to prepare the desired analogs in enantiomerically pure form as the required enantiomerically pure starting material was readily available (Scheme 2). We envisaged that DORA **4** would have a similar receptor binding mode to the known (*S*)-pyrrolidine SB-674042 disclosed by Smithkline Beecham,[47] and we therefore set out to first prepare the (*S*)-enantiomer of our pyrrolidine.[48]

Reaction of prolinol with sulfuryl chloride in pyridine and dichloromethane at −78°C provided the bicyclic sulfamate

Table 2 SAR exploration of the benzyl group

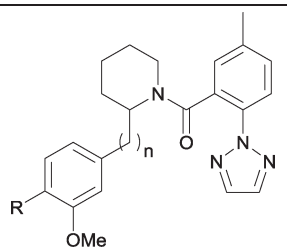

			IC_{50}[a] (nM)		
Cmpd	R	*n*	OX_1	OX_2	HLM[b]
(±) **4**	OMe	1	2.7	3.3	616
(±) **5**	OMe	2	28	16	817
(±) **6**	H	2	108	243	1173

[a] Geomean of at least 3 experiments, standard deviation is <50% in all cases. [b] Intrinsic metabolic clearance (μL min^{-1} mg^{-1}) with human liver microsomes, at 1 μM.

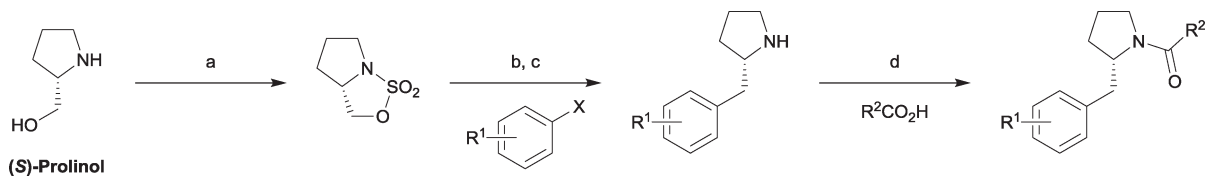

Scheme 2 Representative synthetic route to 1-acyl-2-benzylpyrrolidines. Reagents and conditions: (a) SO_2Cl_2, Py, DCM, −78 °C, 43–71%; (b) *n*BuLi, THF, −78 °C, X = Br or I, 10–95%; (c) H^+, EtOH, 95 °C, 10–95%; (d) TBTU, DIPEA, DMF, RT, 30–90%. For variations of R1 see Tables 3 & 5 and for variations of R2 see Tables 3 & 6.

Table 3 Potency, microsomal stability, and LLE of selected 1-acyl-2-benzylpyrrolidines

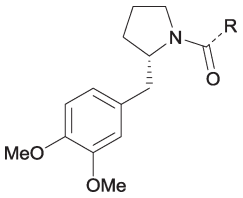

Cmpd	R	IC_{50}[a] (nM) OX_1	OX_2	HLM[b] (RLM[b])	LLE
7	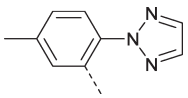	8.5	8.4	356 (>1250)	4.7
8	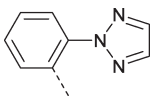	16	3.5	104 (>1250)	5.4
9	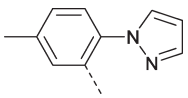	45	65	>1250	3.9
10	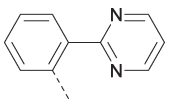	16	4.7	102	4.5
11	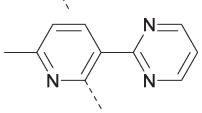	60	71	17	3.8
12	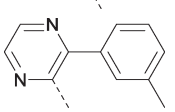	23	4.0	158	4.5
13	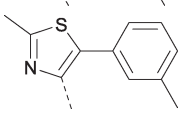	3.5	3.1	338 (>1250)	3.3
14	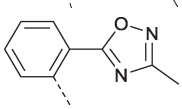	33	12	129	4.0

[a] Geomean of at least 3 experiments, standard deviation is <50% in all cases. [b] Intrinsic metabolic clearance (μL min^{-1} mg^{-1}) with liver microsomes, at 1 μM.

intermediate, that was subsequently reacted with the lithium anion of the chosen benzene derivative. Acidic hydrolysis of the isolated sulfamic acid at an elevated temperature furnished the corresponding 2-benzyl pyrrolidine with intact stereochemical integrity. Amide formation with the required *o*-biaryl carboxylic acid gave the desired compound.

This ring contraction led to compound 7 (Table 3), showing a 6-fold loss in potency at both OX_1 and OX_2 (assuming racemic **4** would be about two times more potent as its active enantiomer). Although the *in vitro* clearance of 7 in RLM remained high (CL_{int} >1250), this structural modification was encouragingly accompanied by a further improvement in metabolic stability in HLM (CL_{int} 356 *vs.* 616). Rat pharmacokinetics were assessed for compound 7, and in line with the measured *in vitro* metabolic stability, this compound had high clearance (55 mL min^{-1} kg^{-1}) and low oral bioavailability (<10%). Nevertheless, physicochemical characteristics were found to be favourable for compound 7, log *D* was determined to be 3, LLE was 4.7, and aqueous solubility was measured as 160 μg mL^{-1} (pH 4.1, unbuffered). Consequently, pyrrolidine 7 demonstrated that the optimisation of physicochemical properties was on track. With the aim to improve pharmacokinetic parameters, the pyrrolidine ring was kept constant in the next round of optimisation and attention turned to the biaryl carboxamide, in particular the tolyl methyl group which was considered a likely metabolic soft spot.

Table 4 Plasma, brain, and CSF exposure 3 h after po dosing to male Wistar rats (n = 3, 100 mg kg^{-1})

Cmpd	Plasma (ng mL^{-1})	Brain (ng g^{-1})	CSF (ng mL^{-1})	B/P ratio
8	114	45	12	0.39
10	737	134	113	0.18
12	225	89	22	0.40
13	129	125	6	0.97

Table 5 Potency, microsomal stability, and LLE of selected 1-acyl-2-benzylpyrrolidines

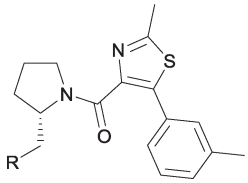

Cmpd	R	IC_{50}[a] (nM) OX_1	OX_2	HLM[b] (RLM[b])	LLE
15	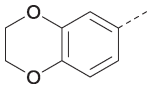	35	39	1040	2.0
16	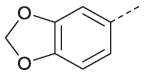	64	40	124	1.9
17	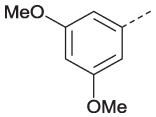	3.4	4.3	798	3.1
18	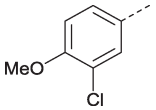	3.8	1.8	>1250 (>1250)	2.8
19	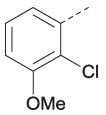	26	16	>1250 (>1250)	1.9
20	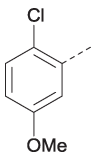	33	18	996 (>1250)	1.8
21	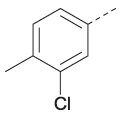	13	10	>1250 (>1250)	1.6
22	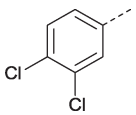	22	66	>1250	0.6

[a] Geomean of at least 3 experiments, standard deviation is <50% in all cases. [b] Intrinsic metabolic clearance (μL min^{-1} mg^{-1}) with liver microsomes, at 1 μM.

Removal of the tolyl methyl group from **7** had little impact on orexin receptor affinity, and in line with expectation, compound **8** showed improved stability in HLM. Disappointingly however, this observation did not translate across species and **8** remained highly unstable in RLM. We next removed one of the triazole nitrogens leading to pyrazole **9** and this resulted in lower potency at both OX receptors. Replacement of the triazole by 2-pyrimidine was well tolerated (**10** *vs.* **8**). Attempts to introduce further polarity such as pyridine **11** resulted in higher microsomal stability albeit with lower potency. Additional heteroaromatic rings were also explored and found to be well tolerated, particularly by OX_2 (**12–14**).

Several structural modifications of the biaryl carboxamide led to an improved stability in HLM, and compounds with CL_{int} values below 100 μL min^{-1} mg^{-1} were even considered too stable for a potential sleep drug. Our next move was to assess central nervous system (CNS) distribution in the rat after oral administration. To circumvent the persistent rat microsomal instability observed so far for this compound class, we opted for high dose experiments with the intention of saturating metabolic processes. Compound concentration was determined in plasma, brain, and cerebrospinal fluid (CSF), the latter being used as a surrogate for brain free concentration. Four compounds were investigated for CNS penetration and all were found to reach low plasma and consequently brain concentrations (Table 4). In terms of brain/plasma ratio, **13** appeared to be the most promising although this compound had the lowest CSF concentration suggesting it was the most highly protein bound.[49,50] Encouraged by the CNS penetration potential of **13**, we selected this compound

Table 6 Potency, microsomal stability, and LLE of selected phenylthiazole carboxamides

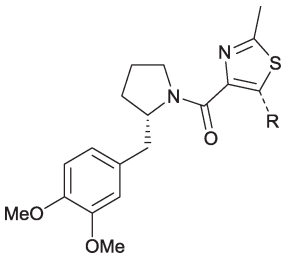

Cmpd	R	IC_{50}[a] (nM) OX_1	OX_2	HLM[b] (RLM[b])	LLE
23	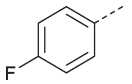	111	62	216	2.2
24	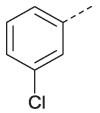	9.1	6.3	612	2.7
25	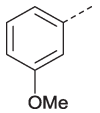	11	7.8	300	3.3
26	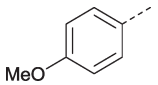	17	10	210	3.2
27	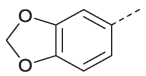	11	6.6	197 (>1250)	3.2
28	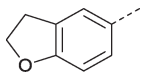	8.3	8.0	235	3.0

[a] Geomean of at least 3 experiments, standard deviation is <50% in all cases. [b] Intrinsic metabolic clearance (μL min^{-1} mg^{-1}) with liver microsomes, at 1 μM.

to explore the dimethoxyphenyl moiety which had largely remained constant during our SAR investigation.

Tethering the two methoxy groups to give compound **15** led to at least a 10-fold loss in potency at both OX receptors and the same was observed for the corresponding piperonyl derivative **16** (Table 5). Relocating the 4-methoxy substituent to the 5-position was well tolerated by the OX receptors but had little influence on microsomal stability as illustrated by **17**. Replacement of the 3-methoxy substituent by chlorine was also well tolerated by both OX receptors albeit with a significant loss of microsomal stability, indicating that **18** had an *in vitro* half-life of less than one minute in the presence of both RLM and HLM. Other structural analogs bearing a chloromethoxy di-substitution pattern as well as 3-chloro,4-methyl and 3,4-dichloro derivatives furnished inferior DORAs with LLE clearly heading in the wrong direction (**19–22**).

Although oxidative demethylation of the dimethoxyphenyl moiety was considered a likely culprit involved in the metabolic turnover of **13**, our SAR investigation into the nature and position of substituents on the phenyl ring provided us with no handle with which to tune metabolic stability. The 3,4-dimethoxy pattern actually turned out to be the most promising when considering both potency and microsomal stability. It is conceivable that the polarity conveyed by the two methoxy groups contributes to lowering the overall lipophilicity of the compound and replacing just one of them is detrimental for metabolic stability.[51] Subsequent attempts to modulate the metabolism were directed back towards the phenylthiazole moiety (Table 6). The 4-fluoro substituted phenyl derivative **23** was not well tolerated by either receptor, resulting in a 32-fold and a 21-fold loss in potency at OX_1 and OX_2, respectively. This motif is present in SB-649868, a clinical compound from GSK which reached phase II trials.[43] The fact that this decoration was not tolerated in our pyrrolidine series implied a different receptor binding mode to the one of the GSK compound. The 3-chloro derivative **24** showed a similar potency to **13**; however, switching methyl for chlorine contributed little to reducing overall lipophilicity. We next explored the 3- and 4-methoxy derivatives **25** and **26**, respectively. Both positions were able to accommodate a methoxy substituent retaining good potency and reasonable stability in HLM. The related piperonyl derivative **27** showed the same profile as either methoxy derivative and replacement of one of the piperonyl oxygen atoms by carbon was well tolerated as illustrated by **28**.

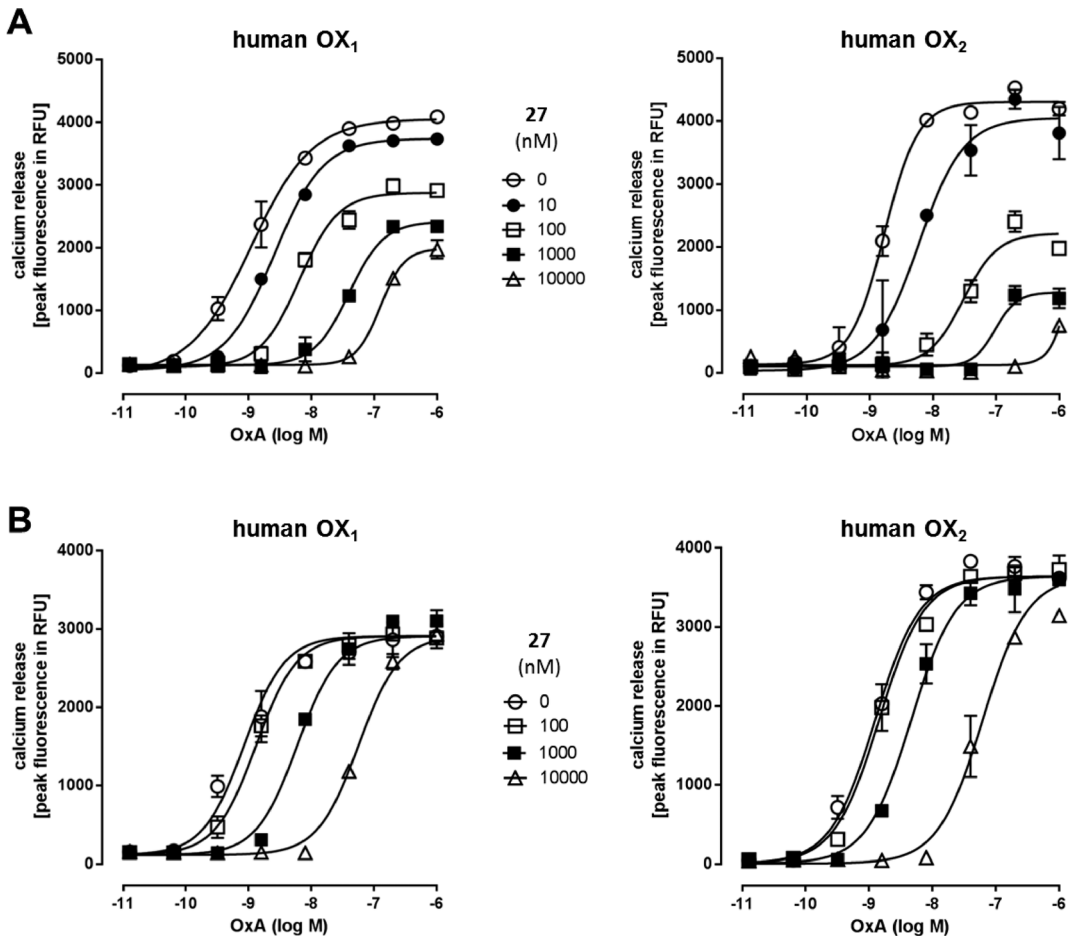

Fig. 1 Effect of **27** on OxA-induced calcium release. (A) CHO cells expressing either the human OX_1 or human OX_2 receptor were pre-incubated with a dilution series of **27** for 120 min followed by the addition of a dilution series of OxA. Calcium release was recorded, peak fluorescence values were exported, and concentration–response curves were generated. IC_{50} values at 1.6 nM OxA were determined and used as a basis to calculate the apparent K_b *via* the generalised Cheng–Prusoff equation. Representative experiment of n = 4 independent experiments is shown. Values represent arithmetic mean of duplicates ±SD. (B) Experiment performed as described in (A) but with simultaneous addition of pre-mixed antagonist and OxA instead of the pre-incubation. Representative experiment of n = 2 independent experiments is shown. Values represent arithmetic mean of duplicates ±SD.

Having made initial efforts to explore the SAR around the 5-phenyl ring of the phenylthiazole moiety, it became clear that in terms of potency several modifications were possible. Piperonyl **27**, showing reasonable human microsomal stability and having an LLE of 3.2, was also measured in RLM and metabolic turnover remained too high to be exactly determined under the chosen assay conditions. The aqueous solubility of **27** was measured as 147 μg mL^{-1} (pH 4.3, unbuffered) indicating that the improvement in solubility for this series of compounds, as already demonstrated for compound **7**, was maintained. Compound **27** was selected for a blood–brain barrier (BBB) experiment under the same conditions already used for **13** (Table 4). To our surprise, plasma concentrations of **27** at 3 h were found to be 2328 ng mL^{-1}, 18-fold higher than those determined for **13**. Brain concentrations were found to be 698 ng g^{-1}, only 6-fold higher than those of **13**, resulting in a total brain/plasma ratio of 0.3 and suggesting that **27** partitions less readily into the CNS as compared to **13**. Unbound fractions in rat plasma and brain[52] were determined *in vitro* to be 2.7% and 4%, respectively, for **27**. As *in vitro* binding data yielded a brain/plasma partition ratio of 0.68, **27** was suspected to be a P-gp substrate in rats. Indeed, **27** exhibited polarised transport in a human P-gp transport assay with an efflux ratio of 7. A brain free fraction of 4% for **27** translated into a free compound concentration of 60 nM, well above its OX_2 IC_{50} value and in line with a measured CSF concentration of 133 ng mL^{-1}.

The mode of antagonism of **27** at OX_1 and OX_2 was assessed in more detail using Ca^{2+} release assays and stably transfected Chinese hamster ovary (CHO) cells recombinantly expressing human or rat OX_1 or OX_2 receptors. Orexin A concentration–response curves (CRC) were generated in the presence of increasing concentrations of **27** (Fig. 1A). The compound induced rightward shifts of the OxA CRCs and a suppression of the maximal OxA response demonstrating insurmountable antagonism. Apparent K_b values (an approximation of the inhibitory constant if IC_{50} values generated at low agonist concentrations are used) were thus calculated

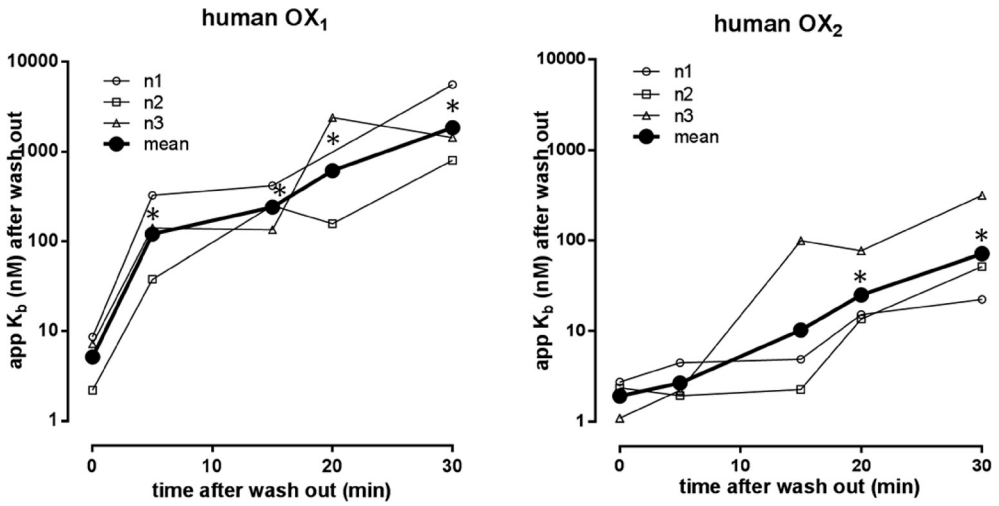

Fig. 2 Dissociation kinetics of **27** determined by calcium release assays in CHO cells expressing either human OX_1 or human OX_2. Cells were pre-incubated for 120 min with antagonist dilution series and then either directly stimulated with OxA (EC_{50}–EC_{70}) or subjected to a compound washout procedure followed by stimulation with OxA at the indicated time points after washout. The peak calcium responses were used to calculate IC_{50} values which were transformed into apparent K_b values as described in the ESI.† The time-dependent changes in apparent K_b after washout of three independent experiments (fine lines) and their geometric mean (bold line) are shown. K_b values after washout that are significantly different ($p < 0.05$) from the K_b at 0 min are indicated with an asterisk. Test: one-way ANOVA, Dunnett's post test.

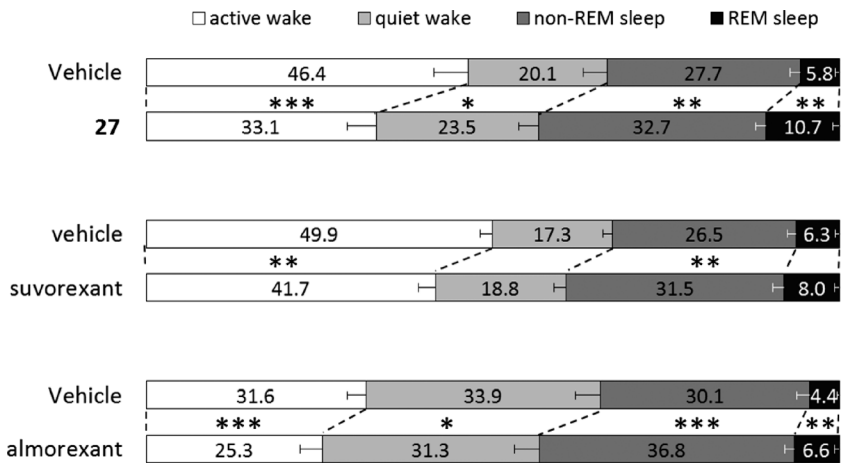

Fig. 3 Effect of **27**, suvorexant, and almorexant on the time spent in sleep and wake stages (% of total time) during the first 6 h of the night active period post administration in male Wistar rats. Rats were administered a single oral dose of vehicle (PEG 400) or 100 mg kg^{-1} of compound. Data are expressed as mean ± SEM. *$p < 0.05$, **$p < 0.01$, ***$p < 0.001$ (n = 8 for **27**, n = 12 for almorexant and n = 14 for suvorexant).

with the help of the generalised Cheng–Prusoff equation as described in the ESI.† Apparent K_b values for 120 min antagonist pre-incubation were calculated to be K_b = 5.3 nM (human OX_1) and 1.4 nM (human OX_2). No differences in potency, selectivity, or surmountability between human and rat receptors were detected.[53]

Insurmountable antagonism can be caused by competitive antagonists with slow dissociation rates as well as by allosteric antagonists that do not compete with the natural ligand for binding but change the affinity for the natural ligand through binding to an allosteric site. These two mechanisms causing insurmountability can be differentiated by performing the previously described curve shift experiments with simultaneous addition of the antagonist dilutions together with the OxA dilutions. In this experimental setting, a competitive binding mode results in antagonist-induced rightward shifts of the OxA CRC without suppression of maximal response, while an allosteric mode of antagonism still results in an insurmountable antagonist profile. Fig. 1B shows the CRCs for OxA in the presence of increasing concentrations of **27** on human OX_1 and OX_2. Clearly, **27** caused rightward shifts in OxA CRCs without suppression of maximal responses demonstrating the competitive nature of its binding mode.

Next, the receptor occupancy half-life ($t_{1/2}$) of **27** at human OX_1 and human OX_2 was assessed using antagonist washout assays in combination with calcium mobilisation assays. CHO cells expressing the recombinant human OX_1 or OX_2

receptors were dyed with fluo-4 and then subjected to a dilution series of **27**. After 120 min of incubation at room temperature, cells were extensively washed to remove all unbound antagonist and then after different recovery times (0–30 min) stimulated with EC_{50-70} of OxA to analyse for residual receptor blockade. The residual blockade was quantified by determining the IC_{50} value at the different time points and then calculating the apparent K_b *via* the generalised Cheng–Prusoff equation using the EC_{50} and slope of the OxA CRC determined at every time point. Three independent experiments were performed. Fig. 2 shows the development of the apparent K_b values after **27** washout. K_b values of the three individual experiments are displayed as fine lines, and their geometric mean is displayed as a bold line. For both receptors, the three experiments yielded similar increases in K_b after washout with a statistically significant change in K_b value *versus* K_b (0 min) occurring at 5 min (OX_1) and at 20 min (OX_2). The fold-change in K_b at these time points was used to calculate an approximate $t_{1/2}$ assuming first-order dissociation kinetics yielding half-lives of 1.1 min (human OX_1) and 5.4 min (human OX_2). For comparison, the half-life of suvorexant was reported to be 79 min at human OX_2.[54] Thus, **27** displays a rather short half-life at OX_1 and OX_2 but long enough to result in insurmountable antagonism in calcium release assays, which represent – due to their rapid response time – the most sensitive assays to detect insurmountable antagonism.

To evaluate the pharmacodynamics of compound **27**, it was tested in a rat sleep model. Male Wistar rats implanted with radiotelemetry probes recording continuously electroencephalogram/electromyography (EEG/EMG) and locomotor activity were administered with a single oral dose of 100 mg kg^{-1} at the beginning of the nocturnal active phase, when endogenous orexin levels increase. DORA **27** showed a comparable sleep-promoting effect to almorexant and suvorexant when tested under the same experimental conditions (Fig. 3). Behaviourally, it significantly decreased home cage activity by 47% over the first 6 h of the night period following administration compared to vehicle-treated animals (−42% and −31% *vs.* vehicle for almorexant and suvorexant at 100 mg kg^{-1} po, respectively, $p < 0.001$ for **27** and almorexant and $p < 0.01$ for suvorexant, paired *t*-test). Electrophysiologically, it decreased significantly the time spent in active wake compared to vehicle-treated animals (−29%, −20% and −16% *vs.* vehicle for **27**, almorexant, and suvorexant, respectively, $p < 0.001$ for **27** and almorexant and $p < 0.01$ for suvorexant, paired *t*-test). Compound **27** increased the time spent in quiet wake by 17% compared to vehicle-treated animals ($p < 0.05$, paired *t*-test). However, the impact on this parameter is not predictive for sleep quality and depends on the compound tested (−8% for almorexant and +9% for suvorexant *vs.* vehicle, $p < 0.05$ and $p > 0.05$, respectively, paired *t*-test). As a consequence of the decrease in time spent in wake stages, the time spent in non-REM (rapid eye movement) sleep was significantly increased *vs.* vehicle over the 6 h period following administration, by +18% for **27**, by +19%, for suvorexant and by +22% for almorexant ($p < 0.01$ for **27** and suvorexant and $p < 0.001$ for almorexant, paired *t*-test). Finally, as observed with other DORAs,[44,55–59] the time spent in REM sleep was also increased compared to vehicle-treated rats, significantly for **27** and almorexant (+84 and +50%, respectively, $p < 0.01$, paired *t*-test) and non-significantly for suvorexant (+20%, $p > 0.05$, paired *t*-test).

Conclusions

In summary, the structural optimisation of a thienopiperidine lead compound led to the discovery of a novel 1-acyl-2-benzylpyrrolidine series of competitive dual orexin receptor antagonists with improved physicochemical properties. Compound **27** showed insurmountable antagonism in calcium release assays at OX_1 and OX_2, combined with a rather short estimated receptor occupancy half-life of 1–5 min at both orexin receptor subtypes. Compound **27** showed a comparable sleep-promoting effect to almorexant and suvorexant when tested under the same experimental conditions. Whilst the potential of the 1-acyl-2-benzylpyrrolidines to deliver *in vivo* active compounds has been demonstrated, further studies shall aim at improving CNS distribution.

Acknowledgements

For expert technical support, the authors gratefully thank Christian Barten, Pauline Schrepfer, Daniel Trachsel, Katalin Menyhart, Celia Müller-Grandjean, Thomas Sasse, Stephane Delahaye, Isabelle Weber, Fabienne Drouet, Eric Soubieux, Rolf Wuest and Julia Friedrich.

Notes and references

1 T. Sakurai, *Nat. Rev. Neurosci.*, 2007, **8**, 171–181.
2 R.-J. Liu, A. N. van den Pol and G. K. Aghajanian, *J. Neurosci.*, 2002, **22**, 9453–9464.
3 T. S. Kilduff and C. Peyron, *Trends Neurosci.*, 2000, **23**, 359–365.
4 L. De Lecea, T. S. Kilduff, C. Peyron, X. B. Gao, P. E. Foye, P. E. Danielson, C. Fukuhara, E. L. F. Battenberg, V. T. Gautvik, F. S. Bartlett II, W. N. Frankel, A. N. Van Den Pol, F. E. Bloom, K. M. Gautvik and J. G. Sutcliffe, *Proc. Natl. Acad. Sci. U. S. A.*, 1998, **95**, 322–327.
5 T. Matsuki and T. Sakurai, *Results Probl. Cell Differ.*, 2008, **46**, 27–55.
6 K. N. Nilaweera, P. Barrett, J. G. Mercer and P. J. Morgan, *Neuroscience*, 2003, **119**, 713–720.
7 T. Sakurai, A. Amemiya, M. Ishii, I. Matsuzaki, R. M. Chemelli, H. Tanaka, S. C. Williams, J. A. Richardson, G. P. Kozlowski, S. Wilson, J. R. S. Arch, R. E. Buckingham, A. C. Haynes, S. A. Carr, R. S. Annan, D. E. McNulty, W.-S. Liu, J. A. Terrett, N. A. Elshourbagy, D. J. Bergsma and M. Yanagisawa, *Cell*, 1998, **92**, 573–585.
8 J. Gatfield, C. Brisbare-Roch, F. Jenck and C. Boss, *ChemMedChem*, 2010, **5**, 1197–1214.
9 R. Spinazzi, P. G. Andreis, G. P. Rossi and G. G. Nussdorfer, *Pharmacol. Rev.*, 2006, **58**, 46–57.

10 K. Yoshida, S. McCormack, R. A. Espana, A. Crocker and T. E. Scammell, *J. Comp. Neurol.*, 2006, **494**, 845–861.
11 M. G. Lee, O. K. Hassani and B. E. Jones, *J. Neurosci.*, 2005, **25**, 6716–6720.
12 J. C. Geerling, T. C. Mettenleiter and A. D. Loewy, *Neuroscience*, 2003, **122**, 541–550.
13 J. Fadel and A. Y. Deutch, *Neuroscience*, 2002, **111**, 379–387.
14 A. Yamanaka, N. Tsujino, H. Funahashi, K. Honda, J.-l. Guan, Q.-P. Wang, M. Tominaga, K. Goto, S. Shioda and T. Sakurai, *Biochem. Biophys. Res. Commun.*, 2002, **290**, 1237–1245.
15 E. Eggermann, M. Serafin, L. Bayer, D. Machard, B. Saint-Mleux, B. E. Jones and M. Muhlethaler, *Neuroscience*, 2001, **108**, 177–181.
16 J. J. Hagan, R. A. Leslie, S. Patel, M. L. Evans, T. A. Wattam, S. Holmes, C. D. Benham, S. G. Taylor, C. Routledge, P. Hemmati, R. P. Munton, T. E. Ashmeade, A. S. Shah, J. P. Hatcher, P. D. Hatcher, D. N. C. Jones, M. I. Smith, D. C. Piper, A. J. Hunter, R. A. Porter and N. Upton, *Proc. Natl. Acad. Sci. U. S. A.*, 1999, **96**, 10911–10916.
17 C. Peyron, D. K. Tighe, A. N. van den Pol, L. de Lecea, H. C. Heller, J. G. Sutcliffe and T. S. Kilduff, *J. Neurosci.*, 1998, **18**, 9996–10015.
18 A. S. Jansen, X. V. Nguyen, V. Karpitskiy, T. C. Mettenleiter and A. D. Loewy, *Science*, 1995, **270**, 644–646.
19 C. J. Winrow, K. Q. Tanis, D. R. Reiss, A. M. Rigby, J. M. Uslaner, V. N. Uebele, S. M. Doran, S. V. Fox, S. L. Garson, A. L. Gotter, D. M. Levine, A. J. Roecker, P. J. Coleman, K. S. Koblan and J. J. Renger, *Neuropharmacology*, 2010, **58**, 185–194.
20 G. C. Harris and G. Aston-Jones, *Trends Neurosci.*, 2006, **29**, 571–577.
21 G. C. Harris, M. Wimmer and G. Aston-Jones, *Nature*, 2005, **437**, 556–559.
22 E. Merlo Pich and S. Melotto, *Front. Neurosci.*, 2014, **8**, 26.
23 P. L. Johnson, W. Truitt, S. D. Fitz, P. E. Minick, A. Dietrich, S. Sanghani, L. Traskman-Bendz, A. W. Goddard, L. Brundin and A. Shekhar, *Nat. Med.*, 2010, **16**, 111–115.
24 M. A. Steiner, H. Lecourt and F. Jenck, *Int. J. Neuropsychopharmacol.*, 2013, **16**, 417–432.
25 M. A. Steiner, H. Lecourt and F. Jenck, *Psychopharmacology*, 2012, **223**, 465–475.
26 T. M. Furlong, D. M. L. Vianna, L. Liu and P. Carrive, *Eur. J. Neurosci.*, 2009, **30**, 1603–1614.
27 B. Boutrel and L. de Lecea, *Physiol. Behav.*, 2008, **93**, 947–951.
28 S. G. Nair, S. A. Golden and Y. Shaham, *Br. J. Pharmacol.*, 2008, **154**, 406–416.
29 C. Brisbare-Roch, J. Dingemanse, R. Koberstein, P. Hoever, H. Aissaoui, S. Flores, C. Mueller, O. Nayler, J. van Gerven, S. L. de Haas, P. Hess, C. Qiu, S. Buchmann, M. Scherz, T. Weller, W. Fischli, M. Clozel and F. Jenck, *Nat. Med.*, 2007, **13**, 150–155.
30 M. Narita, Y. Nagumo, S. Hashimoto, M. Narita, J. Khotib, M. Miyatake, T. Sakurai, M. Yanagisawa, T. Nakamachi, S. Shioda and T. Suzuki, *J. Neurosci.*, 2006, **26**, 398–405.
31 P. J. Coleman, C. D. Cox and A. J. Roecker, *Curr. Top. Med. Chem.*, 2011, **11**, 696–725.
32 P. Hoever, G. Dorffner, H. Benes, T. Penzel, H. Danker-Hopfe, M. J. Barbanoj, G. Pillar, B. Saletu, O. Polo, D. Kunz, J. Zeitlhofer, S. Berg, M. Partinen, C. L. Bassetti, B. Hoegl, I. O. Ebrahim, E. Holsboer-Trachsler, H. Bengtsson, Y. Peker, U. M. Hemmeter, E. Chiossi, G. Hajak and J. Dingemanse, *Clin. Pharmacol. Ther.*, 2012, **91**, 975–985.
33 D. Michelson, E. Snyder, E. Paradis, M. Chengan-Liu, D. B. Snavely, J. Hutzelmann, J. K. Walsh, A. D. Krystal, R. M. Benca, M. Cohn, C. Lines, T. Roth and W. J. Herring, *Lancet Neurol.*, 2014, **13**, 461–471.
34 L. Citrome, *Int. J. Clin. Pract.*, 2014, **68**, 1429–1441.
35 US Belsomra Package Insert. United States Food and Drug Administration product information. Available from: http://www.accessdata.fda.gov/scripts/cder/drugsatfda/index.cfm?fuseaction=Search.Label_ApprovalHistory#labelinfo.
36 C. Dugovic, J. E. Shelton, S. Yun, P. Bonaventure, B. T. Shireman and T. W. Lovenberg, *Front. Neurosci.*, 2014, **8**, 28.
37 A. J. Roecker, S. P. Mercer, J. D. Schreier, C. D. Cox, M. E. Fraley, J. T. Steen, W. Lemaire, J. G. Bruno, C. M. Harrell, S. L. Garson, A. L. Gotter, S. V. Fox, J. Stevens, P. L. Tannenbaum, T. Prueksaritanont, T. D. Cabalu, D. Cui, J. Stellabott, G. D. Hartman, S. D. Young, C. J. Winrow, J. J. Renger and P. J. Coleman, *ChemMedChem*, 2014, **9**, 311–322.
38 S. P. Mercer, A. J. Roecker, S. Garson, D. R. Reiss, C. Meacham Harrell, K. L. Murphy, J. G. Bruno, R. A. Bednar, W. Lemaire, D. Cui, T. D. Cabalu, C. Tang, T. Prueksaritanont, G. D. Hartman, S. D. Young, C. J. Winrow, J. J. Renger and P. J. Coleman, *Bioorg. Med. Chem. Lett.*, 2013, **23**, 6620–6624.
39 C. W. Murray, D. A. Erlanson, A. L. Hopkins, G. M. Keserü, P. D. Leeson, D. C. Rees, C. H. Reynolds and N. J. Richmond, *ACS Med. Chem. Lett.*, 2014, **5**, 616–618.
40 M. Bolli, C. Boss, C. Brotschi, B. Heidmann, T. Sifferlen, D. Trachsel and J. T. Williams, WO2012114252A1, 2012.
41 D. Gramec, L. Peterlin Masic and M. Sollner Dolenc, *Chem. Res. Toxicol.*, 2014, **27**, 1344–1358.
42 P. J. Coleman, J. D. Schreier, C. D. Cox, M. J. Breslin, D. B. Whitman, M. J. Bogusky, G. B. McGaughey, R. A. Bednar, W. Lemaire, S. M. Doran, S. V. Fox, S. L. Garson, A. L. Gotter, C. M. Harrell, D. R. Reiss, T. D. Cabalu, D. Cui, T. Prueksaritanont, J. Stevens, P. L. Tannenbaum, R. G. Ball, J. Stellabott, S. D. Young, G. D. Hartman, C. J. Winrow and J. J. Renger, *ChemMedChem*, 2012, **7**, 415–424.
43 R. Di Fabio, A. Pellacani, S. Faedo, A. Roth, L. Piccoli, P. Gerrard, R. A. Porter, C. N. Johnson, K. Thewlis, D. Donati, L. Stasi, S. Spada, G. Stemp, D. Nash, C. Branch, L. Kindon, M. Massagrande, A. Poffe, S. Braggio, E. Chiarparin, C. Marchioro, E. Ratti and M. Corsi, *Bioorg. Med. Chem. Lett.*, 2011, **21**, 5562–5567.
44 C. D. Cox, M. J. Breslin, D. B. Whitman, J. D. Schreier, G. B. McGaughey, M. J. Bogusky, A. J. Roecker, S. P. Mercer, R. A. Bednar, W. Lemaire, J. G. Bruno, D. R. Reiss, C. M. Harrell, K. L. Murphy, S. L. Garson, S. M. Doran, T. Prueksaritanont, W. B. Anderson, C. Tang, S. Roller, T. D. Cabalu, D. Cui, G. D. Hartman, S. D. Young, K. S. Koblan, C. J. Winrow, J. J. Renger and P. J. Coleman, *J. Med. Chem.*, 2010, **53**, 5320–5332.
45 C. L. Branch, W. N. Chan, A. Johns, C. N. Johnson, D. J. Nash, R. Novelli, J.-P. Pilleux, R. A. Porter, R. E. A. Stead and G. Stemp, WO2003002561A1, 2003.

46 P. D. Leeson and B. Springthorpe, *Nat. Rev. Drug Discovery*, 2007, **6**, 881–890.
47 C. J. Langmead, J. C. Jerman, S. J. Brough, C. Scott, R. A. Porter and H. J. Herdon, *Br. J. Pharmacol.*, 2004, **141**, 340–346.
48 G. F. Cooper and M. G. Martin, US5130432A, 1992.
49 T. T. Mariappan, V. Kurawattimath, S. S. Gautam, C. P. Kulkarni, R. Kallem, K. S. Taskar, P. H. Marathe and S. Mandlekar, *Mol. Pharmaceutics*, 2014, **11**, 477–485.
50 J. Watson, S. Wright, A. Lucas, K. L. Clarke, J. Viggers, S. Cheetham, P. Jeffrey, R. Porter and K. D. Read, *Drug Metab. Dispos.*, 2009, **37**, 753–760.
51 An LCMS retention time shift of 0.07 min was observed for compound **18** *vs.* compound **13**, see the ESI.†
52 K. D. Read and S. Braggio, *Expert Opin. Drug Metab. Toxicol.*, 2010, **6**, 337–344.
53 For a comparison of human *vs.* rat K_b values please see Table S1 in the ESI.†
54 R. Mould, J. Brown, F. H. Marshall and C. J. Langmead, *Br. J. Pharmacol.*, 2014, **171**, 351–363.
55 C. J. Winrow, A. L. Gotter, C. D. Cox, P. L. Tannenbaum, S. L. Garson, S. M. Doran, M. J. Breslin, J. D. Schreier, S. V. Fox, C. M. Harrell, J. Stevens, D. R. Reiss, D. Cui, P. J. Coleman and J. J. Renger, *Neuropharmacology*, 2012, **62**, 978–987.
56 T. Sifferlen, C. Boss, E. Cottreel, R. Koberstein, M. Gude, H. Aissaoui, T. Weller, J. Gatfield, C. Brisbare-Roch and F. Jenck, *Bioorg. Med. Chem. Lett.*, 2010, **20**, 1539–1542.
57 H. Aissaoui, R. Koberstein, C. Zumbrunn, J. Gatfield, C. Brisbare-Roch, F. Jenck, A. Treiber and C. Boss, *Bioorg. Med. Chem. Lett.*, 2008, **18**, 5729–5733.
58 C. Boss, C. Brisbare-Roch, F. Jenck, H. Aissaoui, R. Koberstein, T. Sifferlen and T. Weller, *Chimia*, 2008, **62**, 974–979.
59 T. Sifferlen, R. Koberstein, E. Cottreel, A. Boller, T. Weller, J. Gatfield, C. Brisbare-Roch, F. Jenck and C. Boss, *Bioorg. Med. Chem. Lett.*, 2013, **23**, 3857–3863.